

# Optimized evolution of networks for principle eigenvector localization

Priodyuti Pradhan<sup>1</sup>, Alok Yadav<sup>1</sup>, Sanjiv K. Dwivedi<sup>1</sup> and Sarika Jalan<sup>1,2</sup>

1. *Complex Systems Lab, Discipline of Physics, Indian Institute of Technology Indore, Khandwa Road, Simrol, Indore-453552, India and*

2. *Centre for Biosciences and Biomedical Engineering, Indian Institute of Technology Indore, Khandwa Road, Simrol, Indore-453552, India*

(Dated: April 5, 2019)

Network science is increasingly being developed to get new insights about behavior and properties of complex systems represented in terms of nodes and interactions. One useful approach is investigating localization properties of eigenvectors which have diverse applications ranging from detection of influential nodes to disease-spreading phenomena in underlying networks. In this work, we evolve an initial random network with an edge rewiring optimization technique considering the inverse participation ratio as a fitness function to obtain a network having a localized principle eigenvector and analyze various properties of the optimized networks. We report few special structural features of such optimized networks including an existence of a set of edges which are necessary for the localization, and rewiring only one of them leads to a complete delocalization of the principal eigenvector. We analytically derive a condition on eigenvector entries for changes in the inverse participation ratio values as a function of edge rewiring. The derivation provides an easy method of finding a pair of nodes, rewiring among them lead to an enhancement in the eigenvector localization.

PACS numbers: 89.75.Hc, 02.10.Yn, 5.40.-a

## I. INTRODUCTION

Networks provide a simple framework to understand and predict properties of complex real-world systems by modelling them in terms of interacting units [1]. This framework is particularly successful in explaining various mechanisms behind the emergence of collective behaviors of systems arising due to the local interaction patterns of their components. Principal eigenvector (PEV) corresponding to the maximum eigenvalue of the network's adjacency matrix has been shown to be especially useful in getting insight into the propagation or localization of perturbation in the underlying systems [2]. One key factor of our interest is to understand properties of networks which may help in spreading or restricting perturbation in networks captured by PEV localization [3]. For instance, during a disease outbreak, one will be interested in knowing if the disease will spread through the underlying network leading to the pandemic or will be localized to a smaller section of the network [2, 4]. Similarly, one may be interested in spreading a particular information, for instance, awareness of vaccination at the time of disease outbreak, or may wish to restrict or localize a perturbation like rumour propagation [5].

Furthermore, metal-insulator transition has been extensively studied using Anderson localization in solid-state physics [6] driving an interest to investigate localization transition in complex networks [7–9]. Localization of an eigenvector refers to a state when few components of the vector take very high values while rest of the components take small values. In the current study, we use inverse participation ratio (IPR) to quantify the eigenvector localization [2]. Localization properties of PEV have been shown to provide insight into the propagation of perturbation in mutualistic ecological networks [3], existence of

rare-regions in brain networks [10], and efficient functioning of Google matrix [11]. Recently, eigenvector localization properties of scale-free networks has been related to the scaling parameter [12] as well as use to detect communities in multilayer and temporal networks [13].

Given the wide range of applicability, investigations of localization phenomena of PEV are crucial to study propagation of perturbation in complex systems. Network properties such as presence of hubs, the existence of dense subgraph, and a power-law degree distribution lead to the PEV localization [2, 14]. However, the questions arise; what are the other structural properties that lead to PEV localization? How can one achieve a network having the most or highly localized PEV for a given network size? What are the particular structural properties or local patterns the network corresponding to the most localized PEV has? How can we incorporate these properties to construct PEV (de)localized networks having real-world applications? This Letter demonstrates that localization behavior of PEV does not have a direct correlation with various popular structural properties, rather the optimized network concerning PEV localization possesses a special structural feature. Analytical derivation of change in IPR value with rewiring of the edges provides an easy way to find out the edges which should be rewired for a better localization of the corresponding network.

We construct a network which has a highly localized PEV using an optimization technique for the network evolution. The optimized network achieved thus has a distinctive architecture. We analyze various structural and spectral properties of this optimized network. Interestingly, there exists a set of edges in the optimized network, rewiring any one of them leads to a complete delocalization of the PEV. We analytically derive the condition for change in the IPR value with the edge rewiring.

## II. METHODS

We represent a simple undirected connected network as  $\mathcal{G} = \{V, E\}$ , where  $V = \{v_1, v_2, \dots, v_N\}$  and  $E = \{e_1, e_2, \dots, e_M\}$  represent the set of nodes and edges, where  $N$  and  $M$  denote the size of  $V$  and  $E$ , respectively. The present work restricts to simple networks, i.e. the network without multiple connections and self-loop. We refer  $E^c = \{e_1^c, e_2^c, \dots, e_{(N(N-1)/2)-M}^c\}$  as the set of edges which are not present in  $\mathcal{G}$ . The adjacency matrix ( $A$ ) corresponding to  $\mathcal{G}$  is defined as,  $a_{ij} = 1$  if there is an edge between node  $i$  and  $j$ , otherwise  $a_{ij} = 0$ . Further,  $d_i = \sum_{j=1}^N a_{ij}$  denotes the degree of node  $v_i$  and  $\{d_i\}_{i=1}^N$  stands for the degree sequence of  $\mathcal{G}$ . The spectrum of  $\mathcal{G}$  is a set of eigenvalues  $\{\lambda_1, \lambda_2, \dots, \lambda_N\}$  of  $A$  where  $\lambda_1 \geq \lambda_2 \geq \dots \geq \lambda_N$ , and corresponding eigenvectors are  $\{X_1, X_2, \dots, X_N\}$ . As  $A$  is a real symmetric matrix, all the eigenvalues are real. Moreover,  $A$  is a non-negative matrix and  $\mathcal{G}$  is always connected, hence from the Perron-Frobenius theorem [15], all the entries of PEV are positive. Therefore, for a connected network, PEV is said to be localized when a large number of components take value near to zero and only a few have large values. We quantify the eigenvector localization using the IPR [2] as follows,

$$IPR(X_k) = \sum_{i=1}^N x_i^4 \quad (1)$$

where  $x_i$  is the  $i^{th}$  component of normalized eigenvector,  $X_k$  with  $k \in \{1, 2, \dots, N\}$ , in the Euclidean norm. A delocalized eigenvector with component  $[1/\sqrt{N}, 1/\sqrt{N}, \dots, 1/\sqrt{N}]$  has an IPR value  $1/N$ , whereas a most localized eigenvector with components  $[1, 0, \dots, 0]$  leads to the IPR value equal to 1. For a connected network, IPR value lies between these two extreme values.

For a given  $N$  and  $M$ , our aim is to get a connected network which has the most localized PEV corresponding to the maximum IPR value. For a particular value of  $N$  and  $M$ , if we can enumerate all the possible network configurations, the network corresponding to the maximum IPR value will be our desired network. The number of possible network configurations for a given  $N$  and  $M$  is of the order  $\mathcal{O}(N^{2M})$  [16]. Therefore, we formulate this problem through an optimization technique as follows. Given an input graph  $\mathcal{G}$  with  $N$  vertices,  $M$  edges and a function  $\zeta: \mathfrak{R}^{N \times 1} \rightarrow \mathfrak{R}$ , we want to compute the maximum possible value of  $\zeta(\mathcal{G})$  over all the simple, connected, undirected, and unweighted graph  $\mathcal{G}$ . Thus, we are maximizing the objective function  $\zeta(\mathcal{G}) = IPR(X_1) = x_1^4 + \dots + x_N^4$  subject to the constraints that  $x_1^2 + \dots + x_N^2 = 1$ , and  $0 < x_i < 1$ . We refer the initial network as  $\mathcal{G}_{init}$  and the optimized network as  $\mathcal{G}_{opt}$ .

Starting from an initial connected Erdős-Rényi(ER) random network [15], we use an edge rewiring approach based on a Monte Carlo algorithm to obtain the most op-

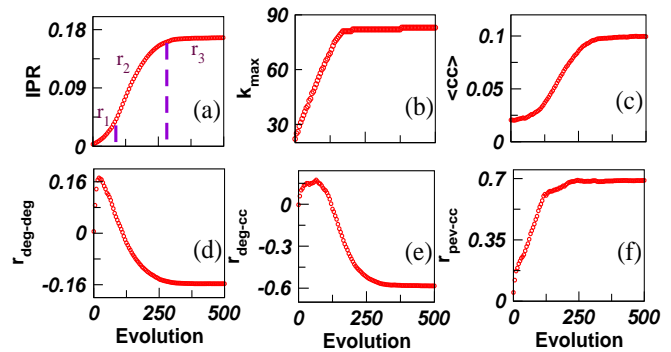


FIG. 1. Network size is  $N = 500$ ,  $\langle k \rangle = 10$  and we iterate the rewiring process for 600,000 times and store the network after each  $100^{th}$  steps. Changes of various network properties (a) IPR value of PEV, (b) maximum degree (c) average clustering coefficient, (d) degree-degree correlation, (e) correlation between degree vector and clustering coefficient vector, and (f) correlation between PEV and clustering coefficient vector during the evolution.

timized network in an iterative manner. For a single edge rewiring process, we choose an edge  $e_i \in E$  uniformly and independently at random from  $\mathcal{G}$  and remove it. At the same time, we introduce an edge in the network from  $E^c$ , which preserves the total number of edges during the network evolution. The new network and the corresponding adjacency matrix are denoted as  $\mathcal{G}'$  and  $A'$ , respectively. The eigenvalues and eigenvectors of  $A'$  are indicated as  $\{\lambda'_1, \lambda'_2, \dots, \lambda'_N\}$  and  $\{X'_1, X'_2, \dots, X'_N\}$ , respectively. It is important to remark that during the network evolution there is a possibility that an edge rewiring makes the network disconnected. We only approve those rewiring steps which yield a connected graph. We calculate the IPR value of PEV from  $A$  and  $A'$ . If  $IPR(X'_1) > IPR(X_1)$ ,  $A$  is replaced with  $A'$ . Therefore, in each time step, we get a network which has the PEV more localized than the previous network. We repeat the above steps, until we obtain the maximum IPR value corresponding to the optimized network,  $\mathcal{G}_{opt}$  (algorithm details in [17]).

## III. RESULTS

Based on the nature of changes in the IPR value as evolution progresses, we can divide the optimization process into three different regions;  $r_1$ ,  $r_2$ , and  $r_3$ , representing slow evolution, fast evolution, and saturation state. Since the total number of edges is fixed throughout the evolution, it is the rearrangements of links which affects the spectral properties of the networks. Moreover, we know that presence of localization affects many structural properties such as the largest degree ( $k_{max}$ ), the average clustering coefficient ( $\langle CC \rangle$ ), degree distribution etc. [2, 9, 14]. We keep a record of all these properties during the evolution and observe that  $k_{max}$  starts rising as IPR value increases with a constant rate and

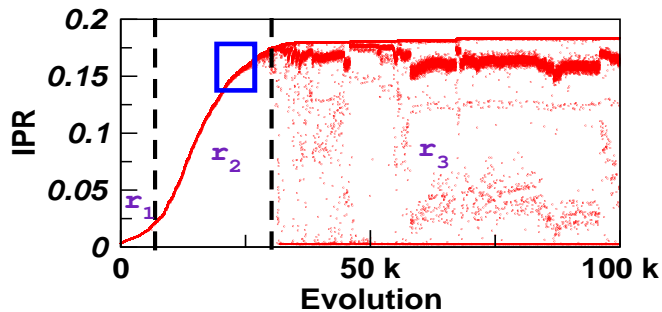


FIG. 2. IPR as a function of edge-rewiring. The networks with large IPR value in  $r_3$  region consists of few edge-rewiring, which leads to a sudden drops in the IPR value. Rewiring of the first 1,00,000 edges is shown. The marked square indicates the regime where the networks attain IPR values which are very close to the optimized network. However, in this regime rewiring an edge does not have a significant impact on the IPR values.

reaches its maximum value much before the IPR achieves its maxima (Fig. 1(b)). This indicates that these two quantities affect each other positively but they are not strongly related. Further to study a possible relation between  $k_{max}$  and IPR value of PEV, we use the configuration model [18] of the  $\mathcal{G}_{opt}$  that has an IPR value which is much smaller than the optimal IPR value, even though both have the same  $k_{max}$  and the degree sequence [17]. This finding indicates that presence of hub node and a particular degree sequence are important for PEV localization. Nevertheless, these may not be the only requirements for achieving a localized PEV and thus we investigate other structural properties which contribute into the localization.

The clustering coefficient is known to play a significant role in localization transition on complex networks [9]. We investigate  $\langle CC \rangle$  vs IPR during the evolution process. We find that as IPR value increases slowly in the  $r_1$  region, while  $\langle CC \rangle$  remains almost constant (Fig. 1(c)). In the  $r_2$  region,  $\langle CC \rangle$  increases rapidly with the evolution and finally gets saturated to a particular value in  $r_3$  region. It suggests that IPR and  $\langle CC \rangle$  have a relation. One possible way to check this relationship is by constructing a network with the same  $\{d_i\}_{i=1}^N$  and  $\langle CC \rangle$  as for  $\mathcal{G}_{opt}$  and to compare the IPR values of both the networks. Interestingly, the network constructed by the algorithm adopted from [19] has IPR value far lesser than the  $\mathcal{G}_{opt}$  [17]. This experiment indicates that regulating  $\langle CC \rangle$  leads to a localization of PEV but it is not as high as  $\mathcal{G}_{opt}$ . Therefore, we investigate other structural properties which might contribute to the PEV localization. One such property is the degree-degree correlation of the networks which we measure using Pearson product-moment correlation coefficient [15].

The degree-degree correlation ( $r_{deg-deg}$ ) during the evolution process exhibits an increment in the beginning when there is a small change in the IPR value ( $r_1$ ) and decreases rapidly with a further increase in IPR value ( $r_2$ ).

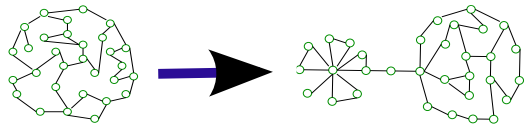


FIG. 3. (Color Online) Schematic diagram representing the initial (left) and the most optimized (right) networks.

Finally, both become saturated (Fig. 1(d)) and  $\mathcal{G}_{opt}$  is a disassortative network. To check the importance of disassortativity for the localization, we perform an experiment by constructing a network using Sokolov algorithm [20] which has the same  $r_{deg-deg}$  as of the  $\mathcal{G}_{opt}$ . However, this construction also fails to yield the IPR value as high as for  $\mathcal{G}_{opt}$  [17]. Further, the degree and clustering coefficient vectors manifest a negative correlation (Fig. 1(e)) whereas local clustering coefficient and PEV indicates a high positive correlation (Fig. 1(f)). These two measurements do provide us information about the possible structure of the networks, but do not tell what the structure exactly is.

#### IV. DISCUSSION

The most intriguing result of our investigation is that we get a special network topology corresponding to the optimized IPR value concerning PEV. The optimized network consists of two components of different sizes which are connected to each other via a single node (Fig. 3). Note that, in between any two increments in IPR values as evolution progresses, there may have several edge rewiring which do not lead to increase in IPR value (algorithm details in [17]). If we consider the rewiring of all the edges, and not only those which lead to an increase in the IPR value, we get surprising results. In the  $r_3$  region (Fig. 2), IPR value gets almost saturated, and there exists only a subtle increment in its value with a further evolution of the network. Though the network in this region has the maximum IPR value, there exists few edges, rewiring them leads to a sudden drop in the IPR value resulting in the complete delocalization of PEV from a highly localized state. It reveals that only a single edge rewiring makes the most localized PEV to delocalized and this phenomenon is observed for sparse networks in  $r_3$  region (Fig. 2), henceforth referred as critical region. We look forward to identify the set of special edges and the rewiring locations, perturbing which, lead to delocalization of PEV. It turns out that in the optimized network if we remove an edge connected to the hub node inside the smaller component (Fig. 3(right)) the IPR value drops down leading to a complete delocalization of PEV. Interestingly, just before the saturation (region  $r_2$ ) if we rewire an edge which is connected to the hub, no sudden drop is observed in the IPR value. This is a region highlighted within a square in (Fig. 2) where IPR value is much larger than the initial ER random network

as well as is robust against the edge rewiring. Whereas in the  $r_3$  region, though the network achieves the maximum IPR value, it becomes very sensitive to the single edge rewiring. Most importantly, by controlling few edges, we can control the PEV localization of the entire network.

We probe deep into finding out the constraints on edge rewiring under which one gets different behaviors of PEV localization so that the framework developed here can be used for various applications. In order to have a comprehensive understanding of the impact of edge rewiring on eigenvector localization, we analytically study the changes in the IPR values and derive the condition which leads to their increment. To proceed, we consider any four distinct arbitrary nodes,  $p, q, r,$  and  $s$  such that there exists an edge between the nodes  $p$  and  $q$  and no edge between  $r$  and  $s$ . As  $A$  is a symmetric matrix, we consider changes in the elements of  $A$ ,  $a_{ij}$  and  $a_{ji}$  simultaneously to measure the variations in the IPR value. During an edge rewiring, value of  $a_{ij}$  flips between 0 and 1. Since  $a_{ij}$  is a discrete variable, changes in  $a_{ij}$  can be defined as  $\Delta a_{ij} = -1(+1)$  for edge removal(edge addition). An edge rewiring is a two-step process; (i) removal of an edge followed by (ii) addition of an edge. The removal of an edge between  $p$  and  $q$  can lead to a change in the IPR value referred as  $\Delta_0 IPR^t$ . Upon adding an edge between  $r$  and  $s$ , there will be changes in the IPR value captured by  $\Delta_1 IPR^{t'}$ . After this two-step rewiring process, the final change in the IPR value will be  $\Delta IPR^{t+1} = \Delta_0 IPR^t + \Delta_1 IPR^{t'}$ . We are interested in the condition causing an increment in the IPR value upon edge rewiring i.e.,

$$\Delta IPR^{t+1} > 0 \quad (2)$$

which we calculate from Eq. 1 as follows,

$$\begin{aligned} \Delta IPR^{t+1} &= IPR^{t+1} - IPR^t \\ &= \sum_{i=1}^N [4(x_i^t)^3 \Delta x_i^{t+1} + 6(x_i^t)^2 (\Delta x_i^{t+1})^2 \\ &\quad + 4x_i^t (\Delta x_i^{t+1})^3 + (\Delta x_i^{t+1})^4] \end{aligned} \quad (3)$$

where  $\Delta x_i^{t+1} = \Delta_0 x_i^t + \Delta_1 x_i^{t'}$  (Detailed derivation provided in SM). Eq. 3 indicates that any changes in the IPR value is governed by the changes in  $x_i$  values. To obtain  $\Delta x_i^{t+1}$ , we use the eigenvalue equation of  $A$ , i.e.  $\sum_{j=1}^N a_{ij}^t x_j^t = \lambda^t x_i^t, \forall i = 1, 2, \dots, N$  which further provides the difference in eigenvector entries before and after the rewiring as (details are in SM);

$$\begin{aligned} \Delta x_i^{t+1} &= \frac{1}{\lambda^t + \Delta \lambda^{t+1}} \left[ \sum_{j=1}^N a_{ij}^t \Delta x_j^{t+1} - \Delta \lambda^t x_i^t + \sum_{j=1}^N (\delta_{jp} \delta_{iq} \right. \\ &\quad \left. + \delta_{jq} \delta_{ip} + \delta_{jr} \delta_{is} + \delta_{js} \delta_{ir}) \Delta a_{ij}^{t+1} (x_j^t + \Delta x_j^{t+1}) \right] \end{aligned} \quad (4)$$

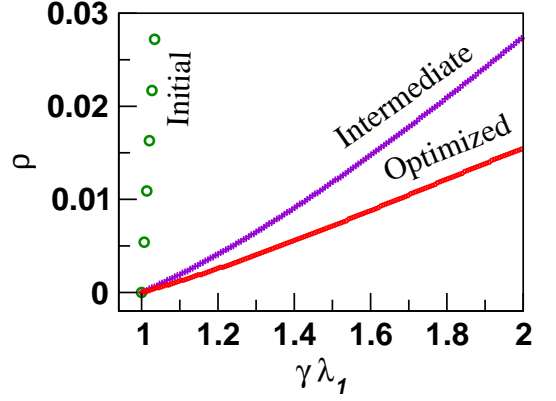


FIG. 4. Spreading process of SIS model on the initial, intermediate (Imdt) and optimized networks have been depicted. Network size and average degree are  $N = 2000$  and  $\langle k \rangle = 10$ , respectively. The largest eigenvalue and IPR value of the corresponding networks are  $\lambda_1(\text{Initial}) = 11.336322$ ,  $IPR(\text{Initial}) = 0.000758$ ,  $\lambda_1(\text{Imdt}) = 11.133781$ ,  $IPR(\text{Imdt}) = 0.200249$  and  $\lambda_1(\text{Optimized}) = 10.773104$ ,  $IPR(\text{Optimized}) = 0.224237$ .

From the numerical experiments, we observe that removal and addition of an edge leads to a minute enhancement in the  $\lambda^t$  value as also reported in Ref. [21], hence we assume  $\lambda^t \approx \lambda^{t+1}$ , where  $\lambda^t$  is the eigenvalue at  $t^{th}$  rewiring steps. Additionally, during the rewiring process  $\Delta x_j^{t+1} \rightarrow 0, \forall j \neq p, q, r, s$ . Hence, to simplify our analysis we assume  $\Delta x_j^{t+1} = 0, \forall j \neq p, q, r, s$  and use Eqs. 3 and 4, we get the expression for changes in IPR values with respect to an edge rewiring as,

$$\begin{aligned} \Delta IPR^{t+1} &= 4 \left[ \frac{\lambda^t x_r^t x_s^t [(x_r^t)^2 + (x_s^t)^2]}{(\lambda^t)^2 - 1} + \frac{[(x_r^t)^4 + (x_s^t)^4]}{(\lambda^t)^2 - 1} \right. \\ &\quad \left. - \frac{x_p^t x_q^t [(x_p^t)^2 + (x_q^t)^2]}{\lambda^t} \right] \end{aligned}$$

By inserting the above equation in the inequality (Eq. 2), we get the condition,  $\frac{\lambda^t x_r^t x_s^t [(x_r^t)^2 + (x_s^t)^2]}{(\lambda^t)^2 - 1} + \frac{[(x_r^t)^4 + (x_s^t)^4]}{(\lambda^t)^2 - 1} > \frac{x_p^t x_q^t [(x_p^t)^2 + (x_q^t)^2]}{\lambda^t}$ . Therefore, during an edge rewiring, if the corresponding PEV entries satisfy the above condition, the rewiring will lead to an enhancement in the IPR value. This condition provides an independent and easy way of finding the pairs of nodes, rewiring process applying on them leads to an increase in IPR value. Hence, just by scanning the eigenvector entries satisfying the above condition, we can create a better localized network. Though the above condition is able to increase the IPR value, but it is further required to elucidate the sudden drops of IPR against the rewiring in the critical region as the current analysis does not explain this phenomenon [17]. Note that the above treatment is applicable for all the eigenvectors and nowhere any assumption is made to restrain the derivation for PEV.

We use standard susceptible-infected-susceptible (SIS)

disease spreading model [2] to analyze the behavior of spreading process on the networks at different steps of the optimization process. In the SIS model, each susceptible vertex becomes infected with the infection rate  $\gamma$  and infected vertices become susceptible with the unit rate. With probability  $\rho_i$ , a vertex  $i$  infected by its neighbours, and prevalence rate is given by  $\rho = \sum_{i=1}^N \rho_i/N$ . We know that when the infection rate  $\gamma$  cross the epidemic threshold i.e.  $\gamma > \gamma_c = \frac{1}{\lambda_1}$  [22] the disease will spread over the networks. However, if the PEV of the network's adjacency matrix is localized, in the vicinity of the epidemic threshold  $\gamma_c + \epsilon$ ,  $\epsilon > 0$  the disease infects a small number of vertices and spreading process becomes slow, and it requires a larger value of  $\gamma$  for spreading of the disease over the network. Fig. 4 manifests that for the initial network just after the  $\gamma_c$ , disease infects a large number of vertices. However, for the intermediate and optimized networks, it infects very few vertices.

## V. CONCLUSION

In this work, starting from an initial random network, we get a network structure through a Monte Carlo based optimization method that possesses highly localized PEV quantified by IPR value. We investigate the optimized network as well as the intermediate networks before the optimized structure is found. In other words, we develop a learning framework to explore localization of eigenvector through a sampling-based optimization method. We analyze several structural properties during the network optimization process. Our analysis identifies a special set of edges which are essential for the (de)localization of PEV in the most optimized network structure. Rewiring

any one edge of this set leads to a complete delocalization of PEV. Moreover, we identify the evolution regime which corresponds to the networks having PEV localization almost same as that of the optimized network but the localization property is robust against the edge rewiring. Eigenvector localization is an important aspect, potentially useful in understanding propagation mechanisms in varied systems such as the virus spread in computer networks [23], vibration confinement systems like spring-mass damping systems and for constructing piezoelectric networks [24, 25]. Another important application of the present study is to have a better understanding of cluster synchronization, a phenomenon observed in a wide range of real-world complex systems, by considering localization properties of eigenvectors of networks Laplacian matrices [26]. Further, the present work focuses on undirected and unweighted networks, the approach can be extended to obtain a comprehensive picture of PEV localization on directed and weighted networks[17]. Furthermore, this Letter is restricted to PEV of adjacency matrices, however it will be interesting to study the consequence of other lower order eigenvectors localization on emerging network properties [27].

## ACKNOWLEDGMENTS

SJ and AY, respectively acknowledge DST, Govt of India grant EMR/2014/000368 and CSIR 09/1022(0013)/2014-EMR-I for financial support. We are thankful to J. N. Bandyopadhyay (BITS-Pilani) for stimulating discussions on eigenvector localizations. We are indebted to Charo I. del Genio (University of Warwick) for several fruitful comments, particularly those related to optimization algorithm and Manavendra Mahato (IIT Indore), Complex Sytems Lab members and Jan Nagler (ETH Zurich) for several useful suggestions.

- 
- [1] Boccaletti S. *et al.*, Phys. Rep. **424**, 175 (2006).
  - [2] A. V. Goltsev *et al.*, Phys. Rev. Lett. **109**, 128702 (2012).
  - [3] S. Suweis *et al.*, Nat. Commun., **6**, 10179 (2015).
  - [4] R. S. Ferreira, R. A. Costa, S. N. Dorogovtsev, and J. F. F. Mendes, Phys. Rev. E **94**, 062305 (2016).
  - [5] D. H. Zanette, Phys. Rev. E **65**, 041908 (2002).
  - [6] P. A. Lee, and T. V. Ramakrishnam, Rev. Mod. Phys. **57**, 287 (1985).
  - [7] V. N. Prigodin and K. B. Efetov Phys. Rev. Lett. **70**, 2932 (1993).
  - [8] M. Ortuño, A. M. Somoza and J. T. Chalker, Phys. Rev. Lett. **102**, 070603 (2009).
  - [9] L. Kahnke *et al.*, Phys. Rev. Lett. **101**, 175702 (2008).
  - [10] P. Moretti, and M. A. Muñoz, Nat. Commun., **4**, 2521 (2013).
  - [11] L. Ermann, K. M. Frahm and D. L. Shepelyansky, Rev. Mod. Phys. **87**, 1261 (2015).
  - [12] R. Pastor-Satorras, and C. Castellano, Sci. Rep. **6**, 18847 (2016).
  - [13] D. Taylor, R. S. Caceres and P. J. Mucha, arXiv:1609.04376v1 (2016).
  - [14] T. Martin, X. Zhang and M. E. J. Newman, Phys. Rev. E **90**, 052808 (2014).
  - [15] M. E. J. Newman, *Networks: An Introduction*, Oxford University Press, (2010).
  - [16] Harary and E. Palmer, *Graphical enumeration*, Academic Press (1973).
  - [17] Supplementary material contains results for scale-free networks, degree and eigenvector distribution plots of ER random networks, and sorted eigenvector entries for the initial and the optimized networks. We have provided numerical results for different network size and average degrees. It also contains all the intermediate steps of the analytical derivation for the discrete case and entire derivation for the continuous case.
  - [18] C. I. D. Genio *et al.*, *PLOS ONE*, **5**, e10012 (2010).
  - [19] L. S. Heath and N. Parikh, Physica A **390**, 4577 (2011).
  - [20] R. X. Brunet and I. M. Sokolov, Phys. Rev. E **70**, 066102 (2004).
  - [21] P. V. Mieghem *et al.*, Phys. Rev. E **84**, 016101 (2011).
  - [22] Y Wang, D Chakrabarti, C Wang and C Faloutsos, Proceedings of the 22nd International Symposium on Reli-

- able Distributed Systems, p. 25 (2003).
- [23] J. Balthrop *et al.*, *Science* **304**, 527 (2004); P. Wang *et al.*, *Science* **324**, 1071 (2009).
- [24] M. A. Rastgaar *et al.*, *J. Sound and Vibration* **329**, 3873 (2010); D. Richiede and A. Trevisani, *Mechanical Systems and Signal Processing* **85**, 556 (2017).
- [25] D. Richiede and A. Trevisani, *Mechanical Systems and Signal Processing* **85**, 556 (2017).
- [26] P. N. McGraw, and M. Menzinger, *Phys. Rev.* **77**, 031102 (2008).
- [27] M. Cucuringu, V. D. Blondel and P. V. Dooren, *Phys. Rev. E* **87**, 032803 (2013).

# Supplementary Data

## Optimized evolution of networks for principal eigenvector localization

Priodyuti Pradhan, Alok Yadav, Sanjiv K. Dwivedi and Sarika Jalan

April 5, 2019

### 1 Introduction

An undirected network with all the eigenvectors associated to an adjacency matrix ( $A$ ) can say to be most localized when a wave-like information, given as an input to a node in the network, is localized or trapped to that node only [1]. In other words, information does not propagate through the network. For instance, if we consider a network where each node is isolated and has only self-loops, the corresponding adjacency matrix will have all its eigenvectors with one entry taking value 1 whereas rest of the entries taking value zero, such as  $[1, 0, \dots, 0]$ . An eigenvector having such entries is referred to as the *most localized* eigenvector. Similarly, an eigenvector represented by  $[1/\sqrt{N}, 1/\sqrt{N}, \dots, 1/\sqrt{N}]$  is said to be a completely delocalized eigenvector. These are two extreme cases for the eigenvector localization. A detailed study on the eigenvector localization and different measurements of localization can be found in Refs. [2, 3].

Furthermore, we can think about the eigenvector localization from a different point of view. We can define a standard basis, i.e.  $\{e_1, e_2, \dots, e_N\}$  in the  $N$  dimensional real vector space where  $e_i \in \mathbb{R}^{N \times 1}$ , with  $i^{th}$  component being equal to 1 and all others being zero. If any eigenvector  $X_j \in \mathbb{R}^{N \times 1}$ ,  $j \in \{1, 2, \dots, N\}$  corresponding to  $A \in \mathbb{R}^{N \times N}$  is aligned with any standard basis vector ( $e_i$ ), we can say that this eigenvector is the most localized one. However, the current investigation considers simple (without self-loop and multiple edges), connected, undirected, and unweighted networks. Therefore, as we know, from the Perron-Frobenius theorem [4], that all the entries of the principal eigenvector (PEV) are positive and it is not possible to achieve an eigenvector which is the most localized. To measure eigenvector localization, we use inverse participation ratio (IPR) value. We focus on studying the localization properties of the largest (principle) eigenvalue and its corresponding eigenvector viz. principal eigenvector and whenever necessary we mention separately about other eigenvectors.

For a particular value of  $N$  (number of nodes) and  $M$  (number of connections), if we can enumerate all the possible network configurations, the network corresponding to the maximum IPR value will be our desired network. The number of possible network configurations for a given  $N$  and  $M$  is of the order  $\mathcal{O}(N^{2M})$  [5]. Therefore, we formulate this problem through an optimization technique as follows. Given an input graph  $\mathcal{G}$  with  $N$  vertices,  $M$  edges and a function  $\zeta : \mathbb{R}^{N \times 1} \rightarrow \mathbb{R}$ , we wish to attain the maximum possible value of  $\zeta(\mathcal{G})$  over all the simple, connected, undirected, and unweighted graph  $\mathcal{G}$ . Thus, we maximize the objective function  $\zeta(\mathcal{G}) = IPR(X_1) = x_1^4 + \dots + x_N^4$  subject to the constraints that  $x_1^2 + \dots + x_N^2 = 1$ , and  $0 < x_i < 1$ . We refer the initial network as  $\mathcal{G}_{init}$  and the optimized network as  $\mathcal{G}_{opt}$ . In the current study, our aim is to get a network having maximum possible IPR value for PEV for a given network size. To the best of our knowledge this is the first piece of work which attempts to construct a network structure having a very high localized PEV for the given network parameters.

We organize the supplementary materials as follows: Section 2 describes the notations and definitions used in the later discussion. In addition, it contains a brief explanation of the optimization procedure used in our work. Section 3 illustrates various numerical results including degree and eigenvector entry distribution of the initial as well as of the optimized network. Moreover, this section exhibits the results for the initial network taken as an SF network. Section 4 consists of analytical derivations of the changes in the IPR value as a function of edge rewiring for discrete as well as continuous cases. Finally, in section 5, we summarize the current study and discuss the open problems for further investigations.

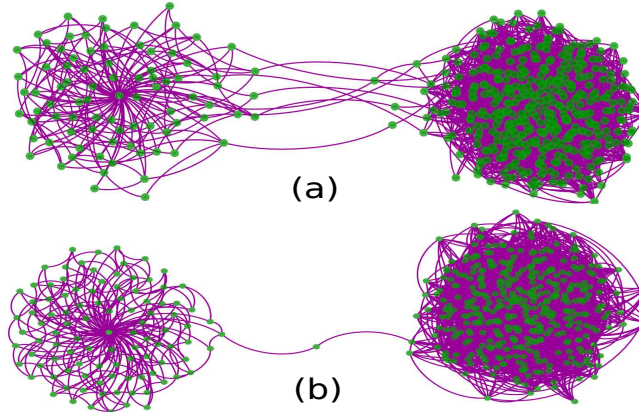


Fig. S 1: cytoscape image from numerical data; Network at (a) intermediate stage of the optimization process (b) the optimized network.

## 2 Methods

We represent our network as  $\mathcal{G} = \{V, E\}$ , for the set of nodes  $V = \{v_1, v_2, \dots, v_N\}$  and edges  $E = \{e_1, e_2, \dots, e_M\}$ , where  $N$  and  $M$  denote the size of  $V$  and  $E$ , respectively. We refer  $E^c = \{e_1^c, e_2^c, \dots, e_{(N(N-1)/2)-M}^c\}$  as the set of edges which are not present in  $\mathcal{G}$ . The adjacency matrix corresponding to  $\mathcal{G}$  is defined as,

$$a_{ij} = \begin{cases} 1 & \text{if } i \sim j \\ 0 & \text{Otherwise} \end{cases}$$

Further,  $d_i = \sum_{j=1}^N a_{ij}$  denotes the degree of node  $v_i$  and  $\{d_i\}_{i=1}^N$  denotes the degree sequence of  $\mathcal{G}$ . We refer  $d$  to be the degree vector and  $\bar{d} = \frac{d}{\sqrt{d^T d}}$  as the normalized degree vector [6]. The *spectrum* of  $\mathcal{G}$  is a set of eigenvalues  $\{\lambda_1, \lambda_2, \dots, \lambda_N\}$  of  $A$  where  $\lambda_1 \geq \lambda_2 \geq \dots \geq \lambda_N$  and corresponding eigenvectors are  $X_1, X_2, \dots, X_N$ , respectively. The new network and the corresponding adjacency matrix after a single edge rewiring can be denoted as  $\mathcal{G}'$  and  $A'$ , respectively. The eigenvalues and eigenvectors of  $A'$  are denoted as  $\{\lambda'_1, \lambda'_2, \dots, \lambda'_N\}$  and  $\{X'_1, X'_2, \dots, X'_N\}$  respectively. We quantify the eigenvector localization using the IPR [7] as follows,

$$IPR(X_k) = \sum_{i=1}^N x_i^4 \quad (1)$$

$$\sum_{i=1}^N x_i^2 = 1 \quad (2)$$

where  $x_i$  is the  $i^{th}$  component of the eigenvector  $X_k$  for  $i, k \in \{1, 2, \dots, N\}$ . Here,  $X_k$ 's are normalized eigenvector in the Euclidean norm.

---

**Algorithm 1: IPR-Optimization**


---

```

1   $ipr \leftarrow IPR(X_1)$  of  $A$ 
2  while  $IPR(X_1)$  not optimized do
3      rewire an edge uniformly and independently at random in  $\mathcal{G}$  and denotes the new
        network as  $\mathcal{G}'$ 
4      check for connectedness of  $\mathcal{G}'$ 
5       $ipr' \leftarrow IPR(X'_1)$  of  $A'$ 
6      if  $ipr' > ipr$  then
7           $A \leftarrow A'$ 
8           $ipr \leftarrow ipr'$ 
9      end
10     store  $ipr$ ,  $ipr'$ , and  $A$ , separately
11 end

```

---

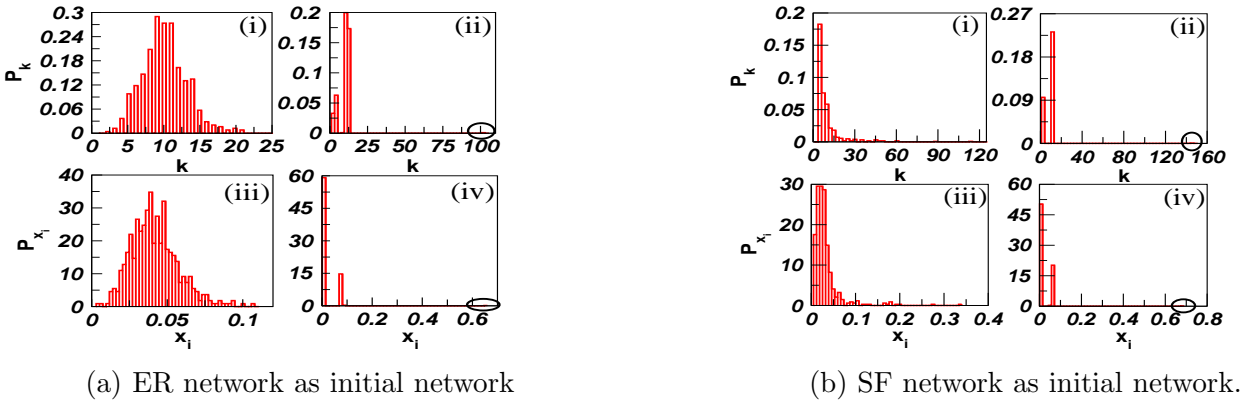


Fig. S 2: Degree distribution of (i) initial network (ii) optimized network; PEV entry distribution of (iii) initial network (iv) optimized network.

The Monte Carlo based optimization process can be summarized as follows. We find PEV ( $X_1$ ), of the adjacency matrix,  $A$  of a graph  $\mathcal{G}$  and calculate the IPR value of  $X_1$ . We rewire one edge uniformly and independently at random in  $\mathcal{G}$  to obtain another graph  $\mathcal{G}'$ . We check whether  $\mathcal{G}'$  is connected, if not the edge rewiring step is repeated till we get another  $\mathcal{G}'$  which is a connected network. We find out PEV of  $A'$  matrix and calculate the IPR value of  $X'_1$ . We replace  $A$  with  $A'$  if  $IPR(X'_1) > IPR(X_1)$ . Steps from third to ten are repeated until IPR value gets saturated which corresponds to the optimized network. We remark that to check the connectedness during an edge rewiring, we use depth-first search (DFS) algorithm [8]. The recorded value of  $ipr$  variable during the optimization process gives the increment of IPR value which is depicted in Fig 1(a) and Fig. S 3(a)(i). Whereas, the recorded value of  $ipr'$  variable during the evolution gives the rewiring of all the edges including drops of the IPR value which is depicted in Fig 2 and Fig. S 3(b). We depict a network at an intermediate evolution stage and the final optimized one in Fig. S 1.

We consider two different network models to create the initial network. One is Erdős-Rényi(ER) model and another is the scale-free (SF) model [9]. The ER random network is generated for edge probability  $p = \frac{\langle k \rangle}{N}$ , where  $\langle k \rangle$  is the average degree of the network. Therefore, in each realization, the total number of edges will fluctuate around  $\frac{N\langle k \rangle}{2}$ , however it does not affect the properties of the final networks evolved through the optimization process. To generate an SF network, we use the Barabasi-Albert model [10].

(a)			(b)			
Index	$ER$	$ER_{opt}$	Index	$ER_{opt}^{conf}$	$ER_{opt}^{cc}$	$ER_{opt}^{r^{deg-deg}}$
$N$	500	500	$N$	500	500	500
$\langle k \rangle$	10	10	$\langle k \rangle$	10	10	10
$N_c$	$2499 \pm 55$	$2499 \pm 55$	$N_c$	$2499 \pm 55$	2499	2499
$k_{max}$	$21 \pm 2$	$90 \pm 7$	$k_{max}$	$90 \pm 7$	100	100
$\lambda_{max}$	$11.04 \pm 0.20$	$11.13 \pm 0.29$	$\lambda_{max}$	$12.67 \pm 0.46$	11.36	11.60
$r^{deg-deg}$	$-0.002 \pm 0.02$	$-0.16 \pm 0.005$	$r^{deg-deg}$	$-0.02 \pm 0.005$	-0.17	-0.16
$IPR$	$0.003 \pm 0.0002$	$0.18 \pm 0.0095$	$IPR$	$0.05 \pm 0.006$	0.02	0.03
$\langle CC \rangle$	$0.02 \pm 0.002$	$0.11 \pm 0.01$	$\langle CC \rangle$	$0.02 \pm 0.003$	0.14	0.01

Table S 1: (a) Results are shown for the average over 31 realizations with 6,00,000 edge rewiring steps.  $ER_{opt}$  denotes the optimized network achieved through the network evolution from the initial base network being  $ER$  network. (b)  $ER_{opt}^{conf}$  refers to the network constructed from the configuration model having the same degree sequence as of the  $ER_{opt}$  network.  $ER_{opt}^{cc}$  refers to the network constructed with the same  $\langle CC \rangle$  and degree sequence as in the  $ER_{opt}$  network. Finally,  $ER_{opt}^{r^{deg-deg}}$  refers to the network having the degree-degree correlation as in the  $ER_{opt}$  network.

### 3 Numerical Results

We have analyzed the degree distribution and PEV entries distribution of the initial as well as optimized networks. During the evolution process, it is observed that there is a drastic change in the degree distribution and distribution of the PEV entries. Moreover, irrespective of whether we start the network optimization process taking ER random network or SF network as an initial network, finally we reach to the network having the same heterogeneous degree distribution (Fig. S 2).

We summarize the ensemble average results for the initial network taken as an ER random network and the optimized network ( $ER_{opt}$ ) in the Table S 1(a). To check the plausible correlation between the degree sequence of the final optimized network and PEV localization, we construct a network which has the same degree sequence as of the optimized network. For this purpose, we use the configuration model [11], which we denote as  $ER_{opt}^{conf}$ . We observe that  $ER_{opt}^{conf}$  has an IPR value which is much lesser than that of the  $ER_{opt}$  network (Table S 1(b)). It concludes that having a specific degree distribution is important but is not the only factor for the PEV localization. Nevertheless, there exist other structural properties which are acquired by the evolved network during the optimization process. In the following, we discuss the impact of other structural properties on the localization of PEV.

Further, we find the clustering coefficient [12] of a node as,

$$C_i = \frac{2\Delta_i}{d_i(d_i - 1)}$$

where  $d_i$  denotes the degree of node  $i$ , and  $\Delta_i$  is the number of triangles the node  $i$  is participating in. Subsequently, the average clustering coefficient [12] can be defined as,

$$\langle CC \rangle = \frac{1}{N} \sum_{i=1}^N C_i$$

During the optimization process, we keep a record of the average clustering coefficient  $\langle CC \rangle$  which indicates an increase in  $\langle CC \rangle$ . To check a correlation between  $\langle CC \rangle$  and IPR, we use an algorithm given in Ref. [13] which takes a degree sequence and average clustering coefficient as an input and creates a random network having the exactly same degree sequence and  $\langle CC \rangle$  as of  $ER_{opt}$ . We denote the network generated using this algorithm as  $ER_{opt}^{cc}$ . It is interesting to observe that

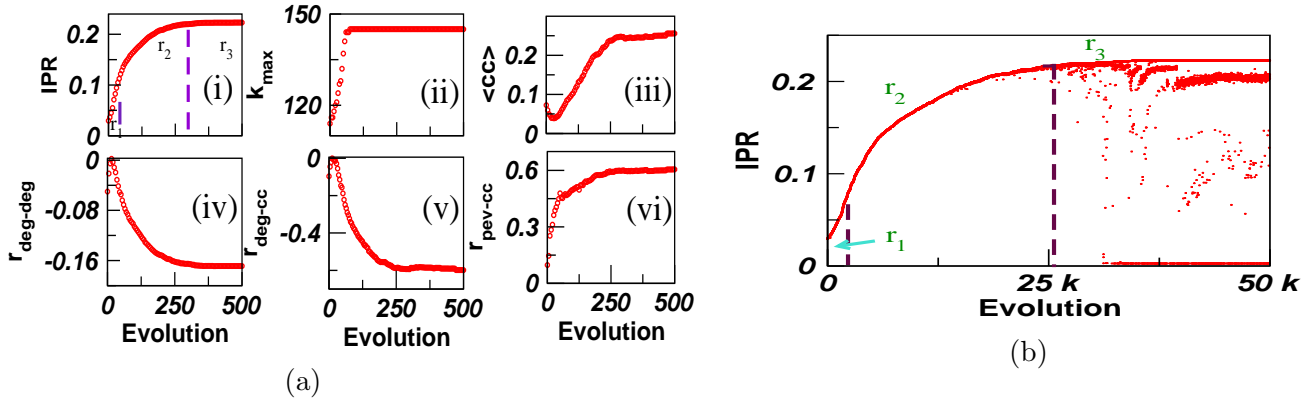


Fig. S 3: (a) Changes of various network properties during the network evolution when initial network is taken as SF network with  $N = 500$ ,  $\langle k \rangle = 10$ . We perform the rewiring process for 2,00,000 edge rewiring steps and store the network after each 100<sup>th</sup> step. Saturated value of IPR fluctuate as  $(0.2 \pm 0.007)$ . (b) In the optimized network, there exists few edges rewiring which lead to a sudden drop in the IPR value.

though  $ER_{opt}$  and  $ER_{opt}^{cc}$  have the same degree sequence and  $\langle CC \rangle$ , they are having different IPR value (Table S 1(b)). It asserts that by tuning  $\langle CC \rangle$ , we cannot achieve a network structure corresponding to  $ER_{opt}$  network. Further, we track the degree-degree correlation coefficient ( $r_{deg-deg}$ ) during the evolution process. The  $r_{deg-deg}$  is measured as follows [14],

$$r_{deg-deg} = \frac{[M^{-1} \sum_{i=1}^M j_i k_i] - [M^{-1} \sum_{i=1}^M \frac{1}{2}(j_i + k_i)^2]}{[M^{-1} \sum_{i=1}^M \frac{1}{2}(j_i^2 + k_i^2)] - [M^{-1} \sum_{i=1}^M \frac{1}{2}(j_i + k_i)^2]}$$

where  $M$  is the total number of edges in the network and  $j_i$ ,  $k_i$  are the degrees of nodes with  $i^{th}$  connection. As a consequence of the evolution process, the  $r_{deg-deg}$  of the optimized network becomes negative indicating the presence of disassortativity in the optimized network. To check how evolution of disassortativity has an impact on the enhancement in the IPR value, we use Sokolov algorithm [15] to construct a network with the same number of  $N$ ,  $M$  and  $r_{deg-deg}$  as in the  $ER_{opt}$  network and is denoted by  $ER_{opt}^{r_{deg-deg}}$ . Again IPR value of the network constructed in this manner is far from the  $ER_{opt}$  network (Table S 1(b)).

Further, we measure the correlation between the clustering coefficient sequence and the PEV entries, using Pearson product-moment correlation coefficient [16]. We measure correlation coefficient between the degree vector and clustering coefficient (cc) vector denoted as  $r_{deg-cc}$  and the correlation between the PEV entries and the cc vector denoted as  $r_{pev-cc}$ .

$$r = \frac{\sum_{i=1}^N (x_i - \bar{x})(y_i - \bar{y})}{\sqrt{\sum_{i=1}^N (x_i - \bar{x})^2} \sqrt{\sum_{i=1}^N (y_i - \bar{y})^2}}$$

To calculate  $r_{deg-cc}$  and  $r_{pev-cc}$ , we normalize the degree vector in the Euclidean norm as in [6]. These measures provide an insight to the network structure of the most optimized network.

In the main article, we have discussed the results of various network properties during the evolution process with an initial network being taken as ER random network. Additionally, herein we consider SF network as an initial network and describe the result in Fig. S 3(a) for changes in various network properties during the evolution with  $N = 500$  and  $\langle k \rangle = 10$ . Fig. S 3(b) exhibits the same IPR pattern as observed for the initial network taken as ER random networks. In fact, if we separate the two components of the optimized network, these do not manifest localized PEV individually. However, these two components taken as  $\mathcal{G}_{init}$  separately, the evolution leads to two optimized networks which have the same structure as in (Fig. 3(right)). However, to achieve a better localized PEV, the network should be sparse. For the dense network, the evolution process

does not lead to a significant increase in the IPR value. The IPR value saturates for a dense network without being appreciably different from the initial network (Fig. 6(b)(i)).

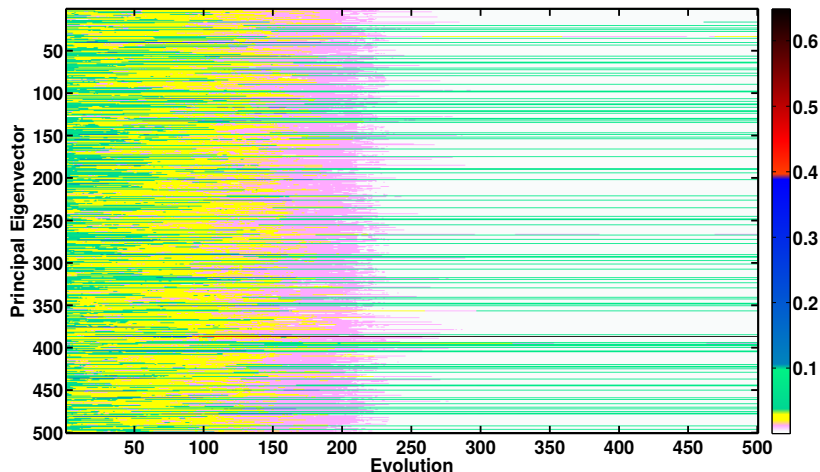


Fig. S 4: Colormap of eigenvector entries during the network evolution of 50,000 iterations. The black color line near 400<sup>th</sup> entry (y-axis) represents the maximum PEV entry weight corresponding to the hub node.

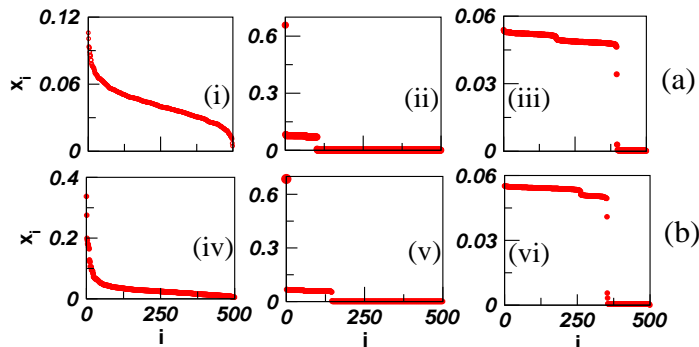


Fig. S 5: Sorted PEV for (i) and (iv) initial ER random and SF network; (ii) and (v) optimized network; (iii) and (vi) after removing an edge connected to hub node.

Furthermore, we scan the eigenvector entries and they provide interesting insight into the final network structure. We depict the changes of the PEV entries during the network evolution using a color map (Fig. S 4). The pictorial representation describes the changes in the PEV entries and formation of the hub node during the evolution. We can see that during the evolution, formation of the hub node happens much before the IPR value gets saturated. Further, we check the sorted PEV entries of  $\mathcal{G}_{init}$ ,  $\mathcal{G}_{opt}$  and  $\mathcal{G}_{opt}^{h-edge}$  whereas  $\mathcal{G}_{opt}^{h-edge}$  is the network obtained after removal of an edge connected to the hub node. After completion of the optimization process, we find a network which has (1) one PEV entry with very high value (2) there exist few relatively smaller entries and, (3) there exists a large chunk of nodes with very small entries (Fig. S 5(ii)). Furthermore, the rewiring which leads to a drop in the IPR value causes a large changes in the PEV entries (Fig. S 5(iii)). The optimized network (localized PEV) and the network obtained after single rewiring (delocalized PEV) differ in only one edge. The sorted PEV corresponding to the initial SF network which has the same pattern as reflects in Fig. S 5(b).

The main article contains the numerical results for several realizations of ER random network with  $N = 500$  and  $\langle k \rangle = 10$ . Here, we provide the results for changes in the IPR values with

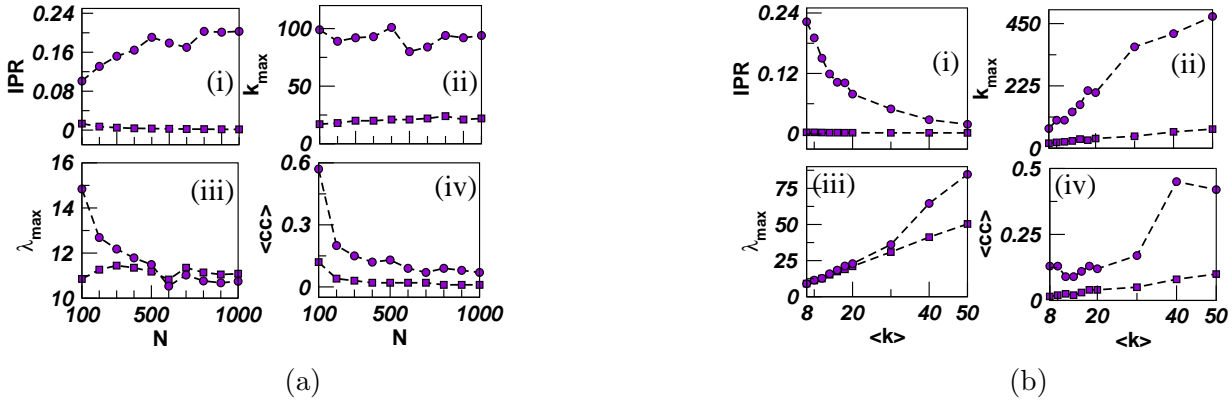


Fig. S 6: Initial network is ER random network; (■) and (●) refer values before and after optimization, respectively. (a) Depicts the results for fixed  $\langle k \rangle = 10$  with different values of  $N$ . (b) Plots for fixed  $N = 500$  with different  $\langle k \rangle$ .

respect to change in  $N$  (Fig. S 6(a)). Furthermore, we observe that as the average degree of the network increases with a fixed  $N$ , IPR value of the final optimized network decreases (Fig. S 6(b)).

## 4 Analytical Derivation

In this section, we present the analytical derivation of the changes in the IPR value as edges are rewired. Our aim is to investigate the changes in the IPR value of a network with respect to an edge rewiring and find out a condition which leads to an increase in the IPR value. Each edge rewiring is a two-step process, (i) removal of an edge followed by (ii) addition of an edge (Fig. S7). Hence, the removal of an edge causes changes in two entries in the adjacency matrix from 1 to 0, and later edge addition changes another two entries from 0 to 1. Thus each edge rewiring changes four entries of the adjacency matrix. Therefore, we consider each  $a_{ij}$  as a discrete variable, however, to make our analysis for a broader class of problems, instead of removing and addition of an edge, we propose to reduce the edge weight by some amount followed by enhancement of similar amount of weight to another edge. For this case,  $a_{ij}$  will not be a discrete variable, rather it will be a continuous variable. First, we consider the case for  $a_{ij}$  being discrete variable and then we consider the continuous case.

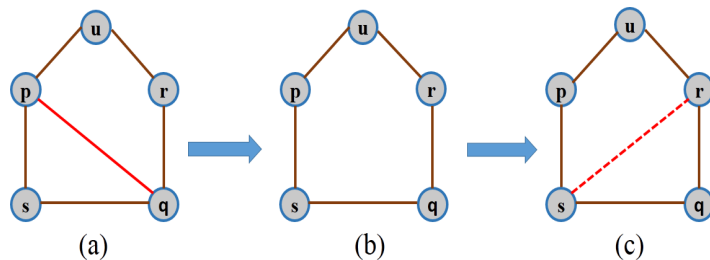


Fig. S 7: Single Edge Rewiring

### 4.1 Derivation for discrete matrix elements

In this section, we analyze how a single edge rewiring lead to a changes in the IPR value. For all the subsequent analysis we consider the symmetric matrix  $A$ , with  $a_{ij} \in \{0, 1\}$ . Given a matrix at  $t^{th}$  step as  $A^t$ , we refer the matrix after a single edge rewiring as  $A^{t+1}$ ,  $t = 0, 1, \dots, T$ , where

$T$  is the total number of edge rewiring during the network evolution or total time step for which the evolution happens. We are interested in the changes of IPR values and hence the eigenvector entries due to a single edge rewiring. We consider four distinct arbitrary nodes  $p, q, r$  and  $s$  such that there exists an edge between  $p$  and  $q$  and no edge between  $r$  and  $s$ . Therefore, we can represent each edge rewiring process as  $A^t \xrightarrow[\Delta a_{qp}]{\Delta a_{pq}} A^{t'} \xrightarrow[\Delta a_{sr}]{\Delta a_{rs}} A^{t+1}$ , where  $A^{t'}$  is the intermediate stage after an edge removal and  $\Delta a_{i,j}$  is the amount of changes caused by a single edge rewiring. Note that during the rewiring, entries corresponding to  $p, q, r$  and  $s$  nodes will change whereas all other entries of  $A^{t+1}$  matrix will remain unchanged. Additionally, in our case,

$$\Delta a_{ij} = \begin{cases} -1 & \text{for edge removal} \\ 1 & \text{for edge addition} \end{cases}$$

But each step will lead to a change in the eigenvalues  $\lambda$  and the corresponding eigenvector entries,  $x_i$ 's. The eigenvalues and eigenvectors of  $A^t$  are denoted as  $\{\lambda_1^t, \lambda_2^t, \dots, \lambda_N^t\}$  and  $\{X_1^t, X_2^t, \dots, X_N^t\}$ , where  $x_i^t$  is the  $i^{th}$  component of the eigenvector  $X_k^t$  for  $k, i \in \{1, 2, \dots, N\}$ . We do not make any assumption in the derivation for a particular eigenvector and the corresponding eigenvalue. Hence, without the loss of generality, we drop  $X_k$  from the IPR notation in Eq. 1 for the rest of the analysis.

Hence, removing an edge lead to a change in two entries of  $A^t$  and produce a new matrix  $A^{t'}$ . We can denote the amount of changes of the eigenvector entries as  $\Delta_0 x_i^{t'}$ , changes in eigenvalue as  $\Delta_0 \lambda_i^{t'}$  and changes in IPR as  $\Delta_0 IPR^{t'}$ . Hence, changes in  $A^{t'}$  will reflect as  $x_i^{t'} = x_i^t + \Delta_0 x_i^{t'}$ ,  $\lambda_i^{t'} = \lambda_i^t + \Delta_0 \lambda_i^{t'}$  and  $IPR^{t'} = IPR^t + \Delta_0 IPR^{t'}$  respectively. Subsequently after adding an edge in  $A^{t'}$  produces  $A^{t+1}$ , and we get another changes as  $\Delta_1 x_i^{t''}$ ,  $\Delta_1 \lambda_i^{t''}$  and  $\Delta_1 IPR^{t''}$ . Hence, the eigenvector entries of  $A^{t+1}$  will be  $x_i^{t+1} = x_i^t + \Delta_0 x_i^{t'} + \Delta_1 x_i^{t''}$ , similarly  $\lambda_i^{t+1} = \lambda_i^t + \Delta_0 \lambda_i^{t'} + \Delta_1 \lambda_i^{t''}$  and  $IPR^{t+1} = IPR^t + \Delta_0 IPR^{t'} + \Delta_1 IPR^{t''}$ . Therefore after the rewiring we have,

$$\begin{aligned} x_i^{t+1} &= x_i^t + \Delta x_i^{t+1}, \text{ where } \Delta x_i^{t+1} = \Delta_0 x_i^{t'} + \Delta_1 x_i^{t''} \\ \lambda_i^{t+1} &= \lambda_i^t + \Delta \lambda_i^{t+1}, \text{ where } \Delta \lambda_i^{t+1} = \Delta_0 \lambda_i^{t'} + \Delta_1 \lambda_i^{t''} \\ IPR^{t+1} &= IPR^t + \Delta IPR^{t+1}, \text{ where } \Delta IPR^{t+1} = \Delta_0 IPR^{t'} + \Delta_1 IPR^{t''} \\ a_{ij}^{t+1} &= a_{ij}^t + \Delta a_{ij}^{t+1} \end{aligned} \quad (3)$$

Note that perturbation theory has been used to measure changes in the eigenvalue and eigenvector of the adjacency matrix of the network with respect to the edge removal and addition [17]. We use the above formulation which gives a way for the subsequent analysis. Our aim is to track the changes in IPR value of a network as edges are rewired and to find out the condition which leads to an increase in the IPR values. The IPR function is given as:

$$IPR^t = \sum_{i=1}^N (x_i^t)^4 \quad (4)$$

Hence, using Eq. 4 we get,

$$\begin{aligned} \Delta IPR^{t+1} &= IPR^{t+1} - IPR^t \\ &= \sum_{i=1}^N (x_i^{t+1})^4 - \sum_{i=1}^N (x_i^t)^4 \\ &= \sum_{i=1}^N (x_i^t + \Delta x_i^{t+1})^4 - \sum_{i=1}^N (x_i^t)^4 \\ &= \sum_{i=1}^N [4(x_i^t)^3 \Delta x_i^{t+1} + 6(x_i^t)^2 (\Delta x_i^{t+1})^2 + 4x_i^t (\Delta x_i^{t+1})^3 + (\Delta x_i^{t+1})^4] \end{aligned} \quad (5)$$

Therefore, any changes in the IPR value (Eq. 5) is governed by the changes in the eigenvector entries. We first measure changes in the eigenvector entries and for that purpose we use the eigenvalue equation as follows,

$$AX = \lambda X$$

At  $t^{\text{th}}$  iterations, we can write using the above equation as follows

$$\sum_{j=1}^N a_{ij}^t x_j^t = \lambda^t x_i^t, \forall i = 1, 2, \dots, N \quad (6)$$

Similarly at  $(t+1)^{\text{th}}$  iterations, it will be,

$$\sum_{j=1}^N a_{ij}^{t+1} x_j^{t+1} = \lambda^{t+1} x_i^{t+1}, \forall i = 1, 2, \dots, N \quad (7)$$

Now, we rewire an edge and measure the changes in the eigenvector entries. Here, we consider separately for  $i = p, q, r,$  and  $s$  nodes and for the rest of other nodes. From Eq. 6 and Eq. 7 we get,

**Case1:**  $i = p$

$$\sum_{j=1}^N a_{pj}^t x_j^t = \lambda^t x_p^t \quad (8)$$

$$\sum_{j=1}^N a_{pj}^{t+1} x_j^{t+1} = \lambda^{t+1} x_p^{t+1} \quad (9)$$

Now we use Eq. 3 in Eq. 9 and get,

$$\sum_{j=1}^N (a_{pj}^t + \Delta a_{pj}^{t+1})(x_j^t + \Delta x_j^{t+1}) = (\lambda^t + \Delta \lambda^{t+1})(x_p^t + \Delta x_p^{t+1})$$

We know that  $a_{pj}^t + \Delta a_{pj}^{t+1} = a_{pj}^t, \forall j \neq q$  and using Eq. 8, we get

$$\Delta x_p^{t+1} = \frac{1}{\lambda^t + \Delta \lambda^{t+1}} \left[ \sum_{j=1}^N a_{pj}^t \Delta x_j^{t+1} - \Delta \lambda^{t+1} x_p^t + \Delta a_{pq}^{t+1} (x_q^t + \Delta x_q^{t+1}) \right]$$

**Case2:** Similarly for  $i = q$

$$\Delta x_q^{t+1} = \frac{1}{\lambda^t + \Delta \lambda^{t+1}} \left[ \sum_{j=1}^N a_{qj}^t \Delta x_j^{t+1} - \Delta \lambda^{t+1} x_q^t + \Delta a_{qp}^{t+1} (x_p^t + \Delta x_p^{t+1}) \right]$$

**Case3:**  $i = r$

$$\Delta x_r^{t+1} = \frac{1}{\lambda^t + \Delta \lambda^{t+1}} \left[ \sum_{j=1}^N a_{rj}^t \Delta x_j^{t+1} - \Delta \lambda^{t+1} x_r^t + \Delta a_{rs}^{t+1} (x_s^t + \Delta x_s^{t+1}) \right]$$

**Case4:**  $i = s$

$$\Delta x_s^{t+1} = \frac{1}{\lambda^t + \Delta \lambda^{t+1}} \left[ \sum_{j=1}^N a_{sj}^t \Delta x_j^{t+1} - \Delta \lambda^{t+1} x_s^t + \Delta a_{sr}^{t+1} (x_r^t + \Delta x_r^{t+1}) \right]$$

**Case5:** and for  $i \neq p, q, r,$  and  $s$

$$\Delta x_i^{t+1} = \frac{1}{\lambda^t + \Delta\lambda^{t+1}} \left[ \sum_{j=1}^N a_{ij}^t \Delta x_j^{t+1} - \Delta\lambda^{t+1} x_i^t \right]$$

In general, combining all of the above five cases by Kronecker delta [9] we get,

$$\Delta x_i^{t+1} = \frac{1}{\lambda^t + \Delta\lambda^{t+1}} \left[ \sum_{j=1}^N a_{ij}^t \Delta x_j^{t+1} - \Delta\lambda^{t+1} x_i^t + \sum_{j=1}^N (\delta_{jp}\delta_{iq} + \delta_{jq}\delta_{ip} + \delta_{jr}\delta_{is} + \delta_{js}\delta_{ir}) \Delta a_{ij}^{t+1} (x_j^t + \Delta x_j^{t+1}) \right]$$

From the numerical simulations we observe that a single edge rewiring makes very small amount of changes in the eigenvalues and also all other entries in the eigenvectors except for  $p, q, r,$  and  $s$  entries. Thus, we assume  $\lambda^t + \Delta\lambda^{t+1} \sim \lambda^t$  and for  $\Delta x_i^{t+1} = 0, \forall i \neq p, q, r,$  and  $s$ . In addition we assume that nodes  $p, q, r,$  and  $s$  are distinct. By using these assumption we get,

$$\begin{aligned} \Delta x_p^{t+1} &= -\frac{x_q^t}{\lambda^t} \\ \Delta x_q^{t+1} &= -\frac{x_p^t}{\lambda^t} \\ \Delta x_r^{t+1} &= \frac{1}{(\lambda^t)^2 - 1} \left( x_s^t \lambda^t + x_r^t \right) \\ \Delta x_s^{t+1} &= \frac{1}{(\lambda^t)^2 - 1} \left( x_r^t \lambda^t + x_s^t \right) \end{aligned} \tag{10}$$

Now, using Eqs. 10 in Eq. 5, we get,

$$\begin{aligned} \Delta IPR^{t+1} &= \left[ 4(x_p^t)^3 \Delta x_p^{t+1} + 6(x_p^t)^2 (\Delta x_p^{t+1})^2 + 4x_p^t (\Delta x_p^{t+1})^3 + (\Delta x_p^{t+1})^4 \right] + \\ &\left[ 4(x_q^t)^3 \Delta x_q^{t+1} + 6(x_q^t)^2 (\Delta x_q^{t+1})^2 + 4x_q^t (\Delta x_q^{t+1})^3 + (\Delta x_q^{t+1})^4 \right] + \\ &\left[ 4(x_r^t)^3 \Delta x_r^{t+1} + 6(x_r^t)^2 (\Delta x_r^{t+1})^2 + 4x_r^t (\Delta x_r^{t+1})^3 + (\Delta x_r^{t+1})^4 \right] + \\ &\left[ 4(x_s^t)^3 \Delta x_s^{t+1} + 6(x_s^t)^2 (\Delta x_s^{t+1})^2 + 4x_s^t (\Delta x_s^{t+1})^3 + (\Delta x_s^{t+1})^4 \right] \end{aligned}$$

As  $\Delta x_i$  is very small, we consider only the first order term and ignore the higher order term and get,

$$\begin{aligned} \Delta IPR^{t+1} &= \left[ 4(x_p^t)^3 \Delta x_p^{t+1} + 4(x_q^t)^3 \Delta x_q^{t+1} + 4(x_r^t)^3 \Delta x_r^{t+1} + 4(x_s^t)^3 \Delta x_s^{t+1} \right] \\ &= 4 \left[ \frac{\lambda^t x_r^t x_s^t [(x_r^t)^2 + (x_s^t)^2]}{(\lambda^t)^2 - 1} + \frac{[(x_r^t)^4 + (x_s^t)^4]}{(\lambda^t)^2 - 1} - \frac{x_p^t x_q^t [(x_p^t)^2 + (x_q^t)^2]}{\lambda^t} \right] \end{aligned}$$

Hence IPR value will increase if the changes of the IPR value  $\Delta IPR^{t+1} > 0$ . Thus,

$$\left[ \frac{\lambda^t x_r^t x_s^t [(x_r^t)^2 + (x_s^t)^2]}{(\lambda^t)^2 - 1} + \frac{[(x_r^t)^4 + (x_s^t)^4]}{(\lambda^t)^2 - 1} \right] > \frac{x_p^t x_q^t [(x_p^t)^2 + (x_q^t)^2]}{\lambda^t} \tag{11}$$

$f_2 > f_1$

where  $f_1 = \frac{x_p^t x_q^t [(x_p^t)^2 + (x_q^t)^2]}{\lambda^t}$  and  $f_2 = \frac{\lambda^t x_r^t x_s^t [(x_r^t)^2 + (x_s^t)^2]}{(\lambda^t)^2 - 1} + \frac{[(x_r^t)^4 + (x_s^t)^4]}{(\lambda^t)^2 - 1}$ . We check our analytical condition (Eq. 11) through numerical experiments. Starting with an ER random network, we

choose a pair of nodes ( $p$  and  $q$ ) such that they have an edge between them and evaluate  $f_1$ . Next, we scan the eigenvector entries ( $x_r$  and  $x_s$ ) by evaluating  $f_2$  such that the above-mentioned inequality holds for it. We check if the nodes corresponding to  $r$  and  $s$  are connected or not. If they are connected, we again scan the other entries such that corresponding nodes are not connected. Once we find two pairs of the nodes satisfying the condition in Eq. 11, we remove the edge between  $p$  and  $q$  and introduce a connection between the nodes  $r$  and  $s$ . We repeat

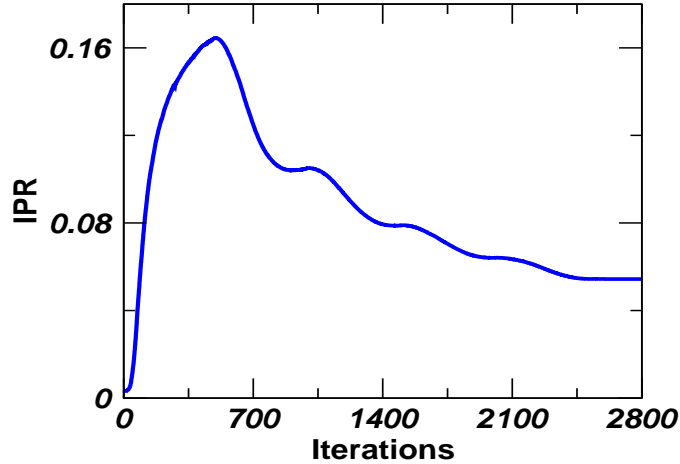


Fig. S 8: Test of analytical results with initial network as ER random network.

this process for a large number of iterations. As reflected from Fig. S 8, initially, satisfying this condition leads to an increment in the IPR value up to 0.16 quite fast. After this value, the rewiring performed based on the pair of eigenvector entries satisfying the condition (in Eq. 11), does not lead to an increase in the IPR value, indeed the IPR value decreases for a further iterations and then it gets saturated (Fig. S 8). It probably happens due to the assumptions made by us, particularly,  $\Delta x_i^{t+1} = 0, \forall i \neq p, q, r,$  and  $s$  (used in Eq. 11). We have observed that our assumptions stand valid for small IPR values ( $r_1$  region) and the regime where IPR values start rapidly increasing (initial part of  $r_2$  region) in Fig. 1(a) and Fig. S3(a)(i). However, during the further evolution, for which the IPR value approaches close to the saturation zone ( $r_3$  region in Fig. 1(a) and Fig. S3(a)(i)), our assumptions do not hold good. Therefore, Eq. 11 is able to provide a condition for the increase in the IPR value but does not give satisfactory conclusion beyond certain regime which requires more investigations. However, it is interesting to note that using the condition in Eq. 11, we achieve 60% of the optimal IPR value within 500 iterations (Fig. S 8), whereas optimization process takes approx. 20,000 iterations to reach it (Fig. 1(a)).

## 4.2 Derivations of Continuous variables

To make the analytical derivation for a large class of problems like instead of removing an edge and adding in another place of the network, we can reduce the edge weight in one place and increase the same amount in another place. Hence, changes will occur in the four entries of the adjacency matrix. Thus, we consider adjacency matrix entries as a continuous variable instead of a discrete variable. It will be applicable for non-negative weighted networks. Here, we reduce the edge weight between the nodes  $p$  and  $q$ , at the same time increase the same amount of edge weight between the nodes  $r$  and  $s$ . To measure the rate of changes in the IPR value with respect to changes in the matrix entry, we differentiate IPR function in Eq. 1 with respect to  $a_{pq}$  and get,

$$\frac{\partial IPR}{\partial a_{pq}} = 4 \sum_{i=1}^N x_i^3 \frac{\partial x_i}{\partial a_{pq}} \quad (12)$$

As  $A$  is a symmetric matrix, we consider the change in  $a_{pq}$  and  $a_{qp}$  entries simultaneously to measure the rate of changes in the IPR value. From Eq. 12, we can say that rate of changes in the IPR value is governed by the rate of changes in the  $x_i$  values. To get the values of  $\frac{\partial x_i}{\partial a_{pq}}$ , we use the eigenvalue equation of  $A$ ,

$$AX = \lambda X$$

which can be written as,

$$\sum_{j=1}^N a_{ij}x_j = \lambda x_i, \quad \forall i = 1, 2, \dots, N \quad (13)$$

Differentiating Eq. 13 with respect to  $a_{pq}$  we get,

$$\lambda \frac{\partial x_i}{\partial a_{pq}} + x_i \frac{\partial \lambda}{\partial a_{pq}} = \sum_{j=1}^N \left[ x_j \frac{\partial a_{ij}}{\partial a_{pq}} + a_{ij} \frac{\partial x_j}{\partial a_{pq}} \right]$$

As mentioned above,  $A$  is a symmetric matrix, so we use

$$\frac{\partial a_{ij}}{\partial a_{pq}} = \left( \delta_{ip}\delta_{jq} + \delta_{iq}\delta_{jp} \right)$$

where  $\delta_{ij}$  is Kronecker delta function [9]. Using the above two equations we get,

$$\lambda \frac{\partial x_i}{\partial a_{pq}} + x_i \frac{\partial \lambda}{\partial a_{pq}} = \delta_{ip}x_q + \delta_{iq}x_p + \sum_{j=1}^N a_{ij} \frac{\partial x_j}{\partial a_{pq}} \quad (14)$$

Further, to calculate the value of  $\frac{\partial \lambda}{\partial a_{pq}}$ , we differentiate Eq. 2 with respect to  $a_{pq}$  and get,

$$\sum_{i=1}^N 2x_i \frac{\partial x_i}{\partial a_{pq}} = 0 \quad (15)$$

We multiply Eq. 13 by  $x_i$  and then differentiate with respect to  $a_{pq}$ , we get

$$2\lambda x_i \frac{\partial x_i}{\partial a_{pq}} + x_i^2 \frac{\partial \lambda}{\partial a_{pq}} = \sum_{j=1}^N \left[ x_i x_j \frac{\partial a_{ij}}{\partial a_{pq}} + a_{ij} x_j \frac{\partial x_i}{\partial a_{pq}} + a_{ij} x_i \frac{\partial x_j}{\partial a_{pq}} \right]$$

Summing over for  $i = 1, 2, \dots, N$  in the above equation and then use Eq. 2 and Eq. 15 we get,

$$\frac{\partial \lambda}{\partial a_{pq}} = 2x_p x_q + \sum_{i=1}^N \sum_{j=1}^N a_{ij} \left[ x_j \frac{\partial x_i}{\partial a_{pq}} + x_i \frac{\partial x_j}{\partial a_{pq}} \right]$$

Using symmetry in the above we get,

$$\frac{\partial \lambda}{\partial a_{pq}} = 2x_p x_q + 2 \sum_{i=1}^N \sum_{j=1}^N a_{ij} x_i \frac{\partial x_j}{\partial a_{pq}} \quad (16)$$

Now we use Eq. 16 in Eq. 14, and get

$$\frac{\partial x_i}{\partial a_{pq}} = \frac{1}{\lambda} \left[ \delta_{ip}x_q + \delta_{iq}x_p - 2x_p x_q x_i + \sum_{j=1}^N a_{ij} \frac{\partial x_j}{\partial a_{pq}} - 2 \sum_{j=1}^N \sum_{k=1}^N a_{jk} x_k x_i \frac{\partial x_j}{\partial a_{pq}} \right] \quad (17)$$

Hence, using Eq. 17 in Eq. 12 we get,

$$\begin{aligned}
\frac{\partial IPR}{\partial a_{pq}} &= \sum_{i=1}^N \frac{4x_i^3}{\lambda} \left[ \delta_{ip}x_q + \delta_{iq}x_p - 2x_px_qx_i - 2 \sum_{k=1}^N \sum_{j=1}^N a_{kj}x_kx_i \frac{\partial x_j}{\partial a_{pq}} + \sum_{j=1}^N a_{ij} \frac{\partial x_j}{\partial a_{pq}} \right] \\
&= \frac{4}{\lambda} \left[ x_qx_p^3 + x_px_q^3 - 2x_px_q \sum_{i=1}^N x_i^4 + \sum_{i=1}^N \sum_{j=1}^N a_{ij}x_i^3 \frac{\partial x_j}{\partial a_{pq}} - 2 \sum_{i=1}^N \sum_{j=1}^N \sum_{k=1}^N a_{kj}x_i^4x_k \frac{\partial x_j}{\partial a_{pq}} \right] \quad (18) \\
&= \frac{4}{\lambda} \left[ x_px_q(x_p^2 + x_q^2 - 2IPR) + \sum_{i=1}^N \sum_{j=1}^N a_{ij}x_i \frac{\partial x_j}{\partial a_{pq}} (x_i^2 - 2IPR) \right]
\end{aligned}$$

From the above equation, we learn that rate of change in the IPR value is inversely proportional to  $\lambda$ , i.e.,  $\frac{\partial IPR}{\partial a_{pq}} \propto \frac{1}{\lambda}$ . Hence, the rate of change in the IPR value will be slow if a network has large  $\lambda$  value. Therefore, Eq. 16, Eq. 17, and Eq. 18 are important which tells about the rate of change in terms of  $\lambda$ ,  $x_i$ , and IPR values.

This enables us to measure the amount of change in the IPR value during and/or after an edge rewiring as follows,

$$IPR \xrightarrow{\partial a_{pq}} IPR + \frac{\partial IPR}{\partial a_{pq}} \varepsilon_1 \xrightarrow{\partial a_{rs}} IPR + \frac{\partial IPR}{\partial a_{pq}} \varepsilon_1 + \frac{\partial IPR}{\partial a_{rs}} \varepsilon_2 + \frac{\partial^2 IPR}{\partial a_{pq} \partial a_{rs}} \varepsilon_1 \varepsilon_2$$

where  $\frac{\partial IPR}{\partial a_{pq}}$  and  $\frac{\partial IPR}{\partial a_{rs}}$  are the rate of changes in the IPR value caused by the change in (p, q) and (r, s) edges, respectively. The amount of changes in the edge weight are denoted by  $\varepsilon_1$  and  $\varepsilon_2$ , respectively. Hence,  $\frac{\partial IPR}{\partial a_{pq}} \varepsilon_1 + \frac{\partial IPR}{\partial a_{rs}} \varepsilon_2 + \frac{\partial^2 IPR}{\partial a_{pq} \partial a_{rs}} \varepsilon_1 \varepsilon_2$  will give the amount of changes in the IPR value for an edge rewiring with  $a_{ij}$  taken as a continuous variable.

## 5 Conclusion and Open Problem

We explore localization properties of the PEV in complex networks. We construct a network structure through the optimization process that possesses highly localized PEV quantified by IPR. We analyze several structural properties during the network optimization process. It suggests that the most localized PEV does not depend upon a single network property rather it depends on several properties simultaneously. This approach provides a comprehensive way to investigate not only the optimized network but also intermediate networks before the most optimized structure is found. In other words, we develop a learning framework to explore localization of eigenvector through a sampling-based optimized method. Additionally, we have identified a special set of edges which are essential for the (de)localization of PEV in the most optimized network structure. Rewiring any one edge belongs to the special set leads to a complete delocalization of PEV. Moreover, we have found a region where networks have a very high localized PEV which is robust against the single edge rewiring. Finally, we have analytically derived a condition for changes in the IPR value as a function of edge rewiring. The condition gives a way to a construct network which has a high localized IPR value for PEV, but using this analytical treatment we can not achieve the IPR value which was observed numerically for the most optimized network. There may exist certain other parameters which should be satisfied to exactly mimic the numerical simulations. Additionally, we have derived the rate of changes in the IPR value for the non-negative weighted symmetric matrices which might be useful to understand the localization in weighted networks.

We have seen that in the saturation time there are drops in the IPR values which leads to the complete delocalization of the PEV. Our analysis also unable to capture such rare phenomenon. We have seen that the edge rewiring leads to the complete delocalization rotating the PEV in approx.  $90^\circ$ . In addition, we find that PEV becomes delocalized and at the same time eigenvector

corresponding to the second largest eigenvalue becomes localized from its delocalized state. Hence, instead of finding the cause of IPR drops, if we can find the reason when small perturbation leads to a large change in the eigen structures, it may give some insight of this IPR drops.

## References

- [1] M. Sade *et al.*, Phys. Rev. E **72**, 066123 (2005).
- [2] P. Cizeau, J. P. Bouchaud, Phys. Rev. E **3**, 1810 (1994).
- [3] C. Bordenave, and A. Guionnet, Probability Theory and Related Fields **157**, 885, (2013).
- [4] P. V. Mieghem, *Graph Spectra for Complex Networks*, Cambridge University Press, (2011).
- [5] F. Harary and E. Palmer, *Graphical enumeration*, 1<sup>st</sup> ed., Academic Press, (1973).
- [6] C. Li , H. Wang and P. V. Mieghem, Networking **7289**, 149, (2012).
- [7] A. V. Goltsev *et al.*, Phys. Rev. Lett. **109**, 128702 (2012).
- [8] T. H. Cormen, C. E. Leiserson, R. L. Rivest, and C. Stein. *Introduction to Algorithms*, 3<sup>rd</sup> ed., MIT Press Cambridge, (2009).
- [9] M. E. J. Newman, *Networks: An Introduction*, Oxford University Press, (2010).
- [10] Réka Albert and Albert-László Barabási, Rev. Mod. Phys. **74**, 47 (2002).
- [11] C. I. D. Genio *et al.*, *PLOS ONE*, **5**, e10012 (2010).
- [12] J. Saramäki *et al.*, Phys. Rev. E **75**, 027105 (2007).
- [13] L. S. Heath, N. Parikh, Physica A **390**, 4577 (2011) .
- [14] M. E. J. Newman, Phys. Rev. Lett. **89**, 208701 (2002).
- [15] R. X. Brunet and I. M. Sokolov, Phys. Rev. E **70**, 066102 (2004).
- [16] D. Freedman, R. Pisani, R. Purves, *Statistics*, 4th ed., W. W. Norton & Company (2007).
- [17] P. V. Mieghem *et. al.*, Phys. Rev. E **84**, 016101 (2011) and references therein.